JACS
JOURNAL OF THE AMERICAN CHEMICAL SOCIETY

ARTICLE

pubs.acs.org/JACS

Mechanically Stabilized Tetrathiafulvalene Radical Dimers

Ali Coskun,[†] Jason M. Spruell,[†] Gokhan Barin,[†] Albert C. Fahrenbach,[†] Ross S. Forgan,[†] Michael T. Colvin,[§,†] Raanan Carmieli,[§,†] Diego Benítez,[‡] Ekaterina Tkatchouk,[‡] Douglas C. Friedman,[†] Amy A. Sarjeant,[†] Michael R. Wasielewski,[§,†] William A. Goddard III,[‡] and J. Fraser Stoddart[†,*]

[†]Department of Chemistry, Northwestern University, 2145 Sheridan Road, Evanston, Illinois 60208, United States

[‡]Materials and Process Simulation Center, California Institute of Technology, Pasadena, California 91125, United States

[§]Argonne-Northwestern Solar Energy Research (ANSER) Center, Northwestern University, Evanston, Illinois 60208, United States

Supporting Information

ABSTRACT: Two donor−acceptor [3]catenanes—composed of a tetracationic molecular square, cyclobis(paraquat-4,4′-biphenylene), as the π-electron deficient ring and either two tetrathiafulvalene (TTF) and 1,5-dioxynaphthalene (DNP) containing macrocycles or two TTF-butadiyne-containing macrocycles as the π-electron rich components—have been investigated in order to study their ability to form TTF radical dimers. It has been proven that the mechanically interlocked nature of the [3]catenanes facilitates the formation of the TTF radical dimers under redox control, allowing an investigation to be performed on these intermolecular interactions in a so-called "molecular flask" under ambient conditions in considerable detail. In addition, it has also been shown that the stability of the TTF radical-cation dimers can be tuned by varying the secondary binding motifs in the [3]catenanes. By replacing the DNP station with a butadiyne group, the distribution of the TTF radical-cation dimer can be changed from 60% to 100%. These findings have been established by several techniques including cyclic voltammetry, spectroelectrochemistry and UV−vis−NIR and EPR spectroscopies, as well as with X-ray diffraction analysis which has provided a range of solid-state crystal structures. The experimental data are also supported by high-level DFT calculations. The results contribute significantly to our fundamental understanding of the interactions within the TTF radical dimers.

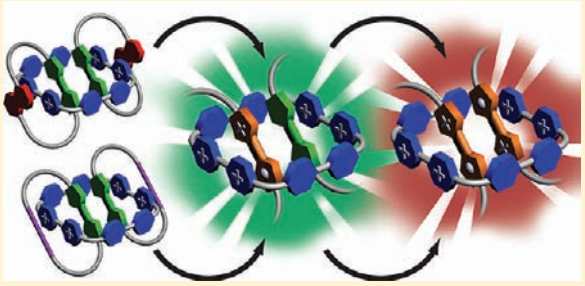

INTRODUCTION

Tetrathiafulvalene (TTF) has received[1] a high level of interest in recent years on account of its unique electrical properties and synthetic versatility.[2] Whereas the neutral form of TTF is a good π-electron donor and has been utilized[3] in the making of switchable mechanically interlocked molecules, it does not exhibit any conducting properties. In 1972, Wudl et al.[4] demonstrated that the radical-cation form of TTF exhibits semiconductor behavior. Thereafter, Ferrais et al.[5] showed that the charge transfer (CT) salt formed between TTF and TCNQ is a narrow band gap semiconductor. To date, studies on this heterocyclic compound have contributed[6] significantly to the development of molecular electronic devices based on these molecules. As a consequence, there have been several attempts to understand[7] the nature of the intermolecular interactions between the different redox states of the TTF units—namely, the TTF mixed-valence dimer $(TTF)_2^{+\bullet}$ (conducting form) and the TTF radical-cation dimer $(TTF^{+\bullet})_2$ (insulating form). However, these dimers are difficult to detect in solution at room temperature on account of their low stabilities—they can be observed[8] only in solution at high concentrations and low temperatures or in the solid state.[7a−7e,7i] Different strategies have been employed to stabilize and study these TTF dimers, namely, (i) covalent attachment[7f,9] of the TTF units in a specific geometry to facilitate the formation of the dimers, and (ii) stabilization of the TTF radical dimers using appropriate host molecules[10] such as cucurbit[8]uril and molecular cages as well as molecular clips. Recently, we have shown that these two strategies can be combined in a [3]catenane[11] and also in a [3]rotacatenane[12] to form robust TTF dimers which are stabilized mechanically within the cavity of a tetracationic molecular square (MS^{4+}) — cyclobis(paraquat-4,4′-biphenylene).[13] The two [3]catenanes $\mathbf{1}^{4+}$ and $\mathbf{2}^{4+}$ (Figure 1) have been shown[11] to form stable, redox-controlled TTF radical dimers, allowing us to probe their structure and spectrophotometric properties in considerable detail under ambient conditions.

Herein, we present a detailed study of the stability of TTF radical dimers in two [3]catenanes (Figure 1) with respect to the mechanism of switching and the effect of the presence of secondary recognition sites which vie for occupancy within the cavity of MS^{4+}. We have shown, by UV−vis−NIR and EPR spectroscopies and cyclic voltammetry in solution, as well as X-ray crystallography and high-level DFT calculations, that (i) the stability of the TTF radical dimers and (ii) the mechanism of switching can be controlled by changing the secondary recognition sites in the [3]catenanes. The results suggest that the unique structures of these mechanically interlocked molecules facilitate

Received: November 24, 2010
Published: March 02, 2011

dx.doi.org/10.1021/ja110584c | J. Am. Chem. Soc. 2011, 133, 4538–4547

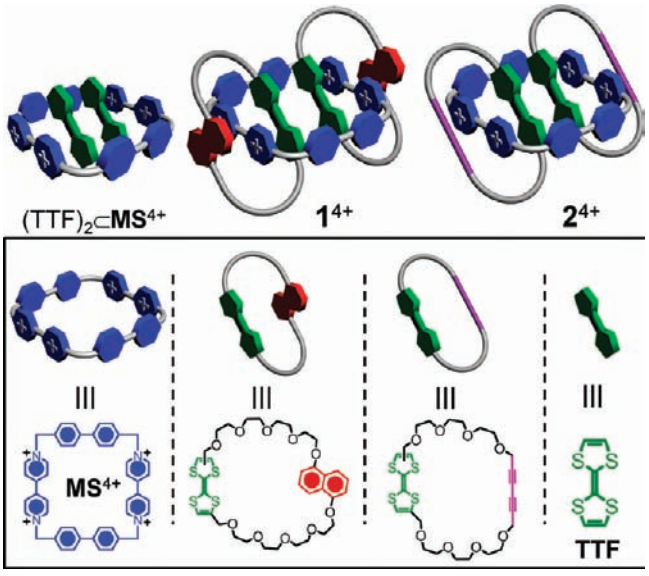

Figure 1. Graphical representations of the inclusion complex $(TTF)_2 \subset \mathbf{MS}^{4+}$, and the [3]catenanes $\mathbf{1}^{4+}$ and $\mathbf{2}^{4+}$ and the corresponding structural formulas for the tetracationic cyclophane $\mathbf{MS}^{4+}$, the macrocyclic polyethers, and the TTF unit. The counterions are PF_6^-.

the formation of the TTF dimers, held together by virtue of mechanical bonds. It is worth noting that, by itself, $\mathbf{MS}^{4+}$ is not a good host for the formation of TTF radical dimers in a supramolecular complex. These results not only provide a fundamental understanding of the properties of these dimers, but they also afford us the opportunity to develop molecular electronic devices with enhanced information storage/processing capacities.

RESULTS AND DISCUSSION

Donor−acceptor bistable [2]catenanes,[3b,6a] containing TTF and 1,5-dioxynaphthalene (DNP) units as the electron-rich stations and cyclobis(paraquat-*p*-phenylene)[14] ($CBPQT^{4+}$) as the electron-deficient cyclophane, have been proven[6a] to be effective molecular switches. In the ground state co-conformation (GSCC), the $CBPQT^{4+}$ ring binds preferentially to the TTF unit rather than to the DNP station. Oxidation of the TTF unit to its radical cation or dication results in Coulombic repulsion leading to the circumrotation of the $CBPQT^{4+}$ ring such that it resides on the DNP station. Upon reduction of the TTF^{2+} dication back to its neutral form, the $CBPQT^{4+}$ ring remains encircled momentarily on the DNP site, populating the so-called metastable state co-conformation (MSCC), before relaxing back to the GSCC. This mechanostereochemical system[15] has been studied and utilized in the fabrication of molecular electronic devices.[6a] On expanding the $CBPQT^{4+}$ ring by replacing the two *p*-xylylene links with bitolyl units, a tetracationic molecular square $\mathbf{MS}^{4+}$—an electron-deficient cyclophane that can form inclusion complexes with two π-electron rich guest molecules—is obtained. This molecular flask enables us to study the guest−guest as well as guest−host interactions within the cavity of the cyclophane. In order to study both $TTF\cdots\mathbf{MS}^{4+}$ and $TTF\cdots TTF$ interactions in (i) the ground state ($TTF\cdots TTF$), (ii) the mixed-valence dimer $(TTF)_2^{+\bullet}$, and (iii) the radical-cation dimer $(TTF^{+\bullet})_2$, all located within the cavity of the tetracationic cyclophane, we have designed (Figure 1) and synthesized, in addition to $\mathbf{MS}^{4+}$, the two [3]catenanes $\mathbf{1}^{4+}$ and $\mathbf{2}^{4+}$. The solution state structural characterization of the inclusion complex $(TTF)_2 \subset \mathbf{MS}^{4+}$ and the two [3]catenanes have been reported[11] by us elsewhere.

In order to probe the mechanically interlocked structures of these two [3]catenanes, we have grown single crystals of both $\mathbf{1}^{4+}$ and $\mathbf{2}^{4+}$ by slow vapor diffusion of *i*-Pr_2O into MeCN solutions of the [3]catenanes at 0 °C. The solid-state structures (Figure 2) of $\mathbf{1}^{4+}$ and $\mathbf{2}^{4+}$ are stabilized by $[\pi\cdots\pi]$ stacking[16] and $[C-H\cdots O]$ interactions.[17] In each [3]catenane, the cavity of MS^{4+} is occupied by the two TTF units, both of which adopt the *trans* configuration and are distorted from planarity in order to maximize the noncovalent bonding interactions between both the TTF units and the polyether loops with the neighboring bipyridinium ($BIPY^{2+}$) moieties. The interplanar separations between the encapsulated TTF units and the plane of the $BIPY^{2+}$ units range from 3.33 to 3.58 Å. In addition, the DNP units in $\mathbf{1}^{4+}$ participate in side-on $[\pi\cdots\pi]$ stacking interactions with the $BIPY^{2+}$ moieties an interplanar distance of 3.49 Å. In agreement with previously reported[18] butadiyne-containing catenanes, the butadiyne units in $\mathbf{2}^{4+}$ align themselves parallel to the $BIPY^{2+}$ moieties with an interplanar separation of 3.64 Å. The distance between the TTF units within the cavity in each case is close to 3.70 Å, suggesting that, in the GSCC, the TTF units interact preferentially with the $BIPY^{2+}$ moieties of the host, rather than with each other. These results suggest, however, that the alignment of the TTF units within the cavity of the tetracationic cyclophane is suited perfectly to the formation of TTF radical dimers, thus allowing us to study these intermolecular interactions within the molecular flask.

To probe the formation of TTF radical dimers upon oxidation of both [3]catenanes, we have performed (Figure 3) UV−vis−NIR spectroscopy experiments[19] at room temperature in which the solutions of both catenanes (c = 0.3 mM in MeCN) were titrated against the oxidant $Fe(ClO_4)_3$. In the ground state, the spectra for both structures exhibit a characteristic TTF-$BIPY^{2+}$ CT absorption band at 905 nm. Upon addition of 1.0 equiv of

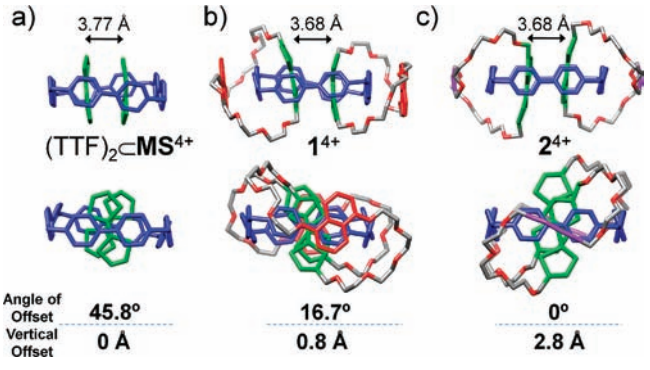

Figure 2. Solid-state (super)structures of (a) the inclusion complex $(TTF)_2 \subset \mathbf{MS}^{4+}$, (b) $\mathbf{1}^{4+}$, and (c) $\mathbf{2}^{4+}$ in stick representation. In all cases, the TTF units are distorted from planarity in order to maximize their interactions with the neighboring $BIPY^{2+}$ units. The distance between two TTF units (ca. 3.70 Å) in each case indicates that they do not interact with each other in the ground state. The angle of offset is defined by the relative orientations of the C−C double bonds in the TTF units: when these bonds are eclipsed the angle is 0°. The vertical offset is the measure of offset between the planes of the TTF units: when these TTF units are in register, the vertical offset value is 0 Å. The hydrogen atoms and counterions have been omitted for clarity.

dx.doi.org/10.1021/ja110584c |*J. Am. Chem. Soc.* 2011, 133, 4538–4547

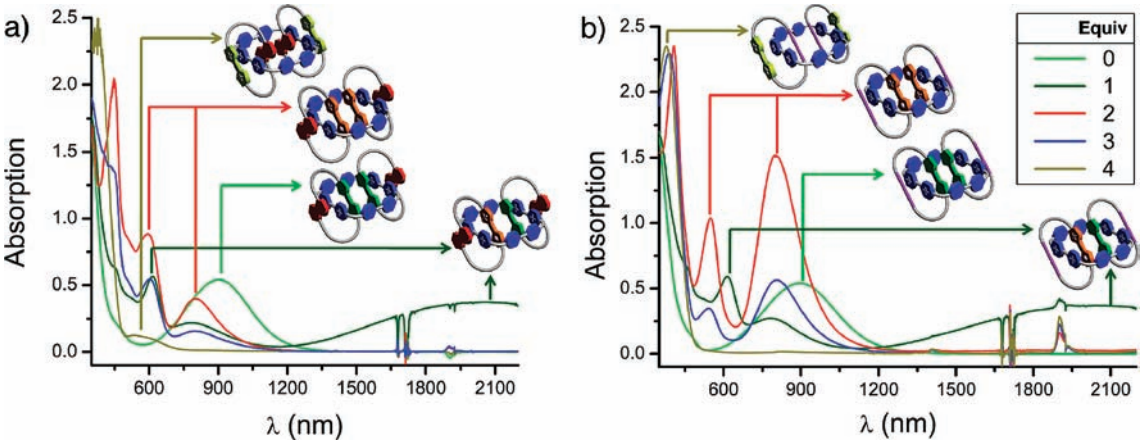

Figure 3. UV−vis−NIR spectra of the [3]catenanes (a) $\mathbf{1}^{4+}$ and (b) $\mathbf{2}^{4+}$ (0.3 mM in MeCN, 10 mm path length, at 298 K) recorded upon addition of up to 4.0 equiv of $Fe(ClO_4)_3$. Both ground states of $\mathbf{1}^{4+}$ and $\mathbf{2}^{4+}$ exhibit TTF-$BIPY^{2+}$ charge transfer (CT) bands at 905 nm. Upon addition of 1.0 equiv of oxidant, formation of characteristic broad NIR bands at 2000 nm for the mixed-valence states was observed. Characteristic absorption bands associated with radical-cation dimer formation were observed at 800 nm. The addition of the oxidant up until generation of the fully oxidized states results in a sharp absorption band corresponding to the TTF^{2+}dication at 375 nm, as well as a band at 600 nm resulting from the CT interaction between DNP and $BIPY^{2+}$ in the case of the fully oxidized form of the [3]catenane $\mathbf{1}^{4+}$.

oxidant, both [3]catenanes $\mathbf{1}^{4+}$ and $\mathbf{2}^{4+}$ displayed a characteristic broad NIR band at 2000 nm, indicating the formation of the mixed-valence state, along with the $TTF^{+\bullet}$ absorption band at 600 nm. Addition of 2.0 equiv of the oxidant resulted in the formation of the radical-cation dimer state $(TTF^{+\bullet})_2$ with the characteristic absorption band observed at 800 nm. The addition of the oxidant up until the fully oxidized states were obtained, resulted in a sharp absorption band corresponding to the TTF^{2+} dication at 375 nm. In addition, a broad absorption at 600 nm in the case of $\mathbf{1}^{4+}$ is associated with CT interactions between the DNP units and $BIPY^{2+}$, indicating the circumrotation of the ring component.

We have carried out (Figure 4a) cyclic voltammetry (CV) experiments in MeCN (electrolyte = 0.1 M $TBAPF_6$) under ambient conditions in order to shed further understanding on the switching characteristics of $\mathbf{1}^{4+}$ and $\mathbf{2}^{4+}$ with reference to the 2:1 inclusion complex $(TTF)_2\subset\mathbf{MS}^{4+}$. To begin with, we investigated the 2:1 inclusion complex $(TTF)_2\subset\mathbf{MS}^{4+}$ in MeCN. There were, however, no significant shifts observed in both the first and second oxidation potentials of the TTF unit

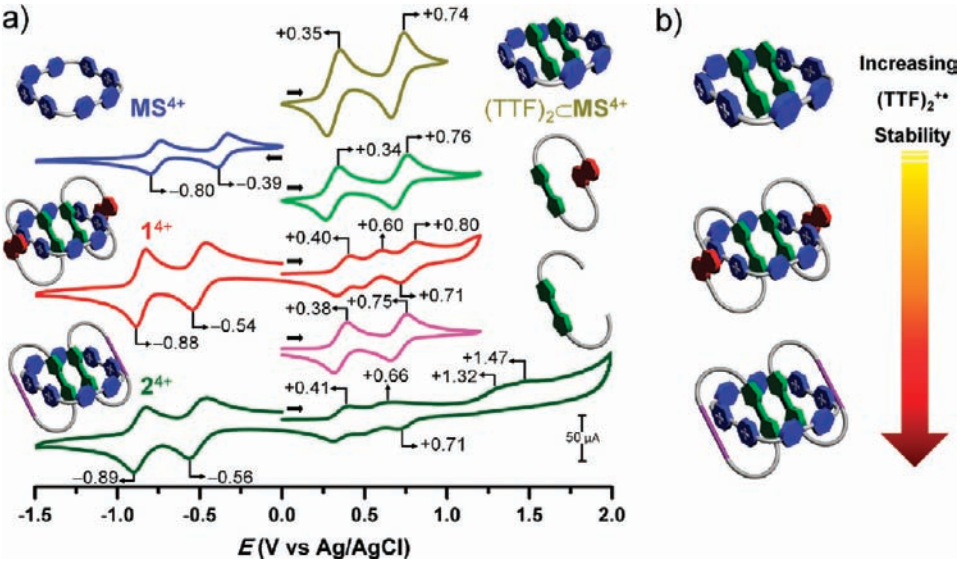

Figure 4. (a) CV traces of the inclusion complex $(TTF)_2\subset\mathbf{MS}^{4+}$ (dark yellow) and the [3]catenanes $\mathbf{1}^{4+}$ (red) and $\mathbf{2}^{4+}$ (dark green) as well as the tetracationic cyclophane $\mathbf{MS}^{4+}$ (blue), the bistable macrocycle (green), and the triethyleneglycol bis-functionalized TTF compound (pink). All spectra were recorded in argon-purged MeCN (1 mM, 0.1 M $TBAPF_6$, 200 mV s^{-1}) at 298 K. The CV of the inclusion complex is very similar to that of a free TTF unit, indicating the absence of formation of TTF radical dimers. The oxidative region of the cyclic voltammogram for $\mathbf{1}^{4+}$ displays three oxidation peaks, pointing to a sequence of one- (+400 mV), one- (+600 mV), and two-electron (+800 mV) processes. In the case of $\mathbf{2}^{4+}$, in which the DNP units have been replaced with butadiyne subunits, the oxidative region shows four one-electron processes occurring with peak potentials at +410, +660, +1320, +1470 mV. The first two oxidations in both [3]catenanes result in the formation of mixed-valence and radical-cation dimer states, respectively. In contrast with $\mathbf{1}^{4+}$, the third and the fourth oxidation peaks for $\mathbf{2}^{4+}$ are shifted to significantly higher potentials, an indication of the formation of a highly stable $(TTF^{+\bullet})_2$ dimer. (b) Diagram summarizing the stability of TTF radical-cation dimers from the inclusion complex to the two [3]catenanes $\mathbf{1}^{4+}$ and $\mathbf{2}^{4+}$.

dx.doi.org/10.1021/ja110584c |*J. Am. Chem. Soc.* 2011, 133, 4538–4547

compared to that of the control compounds, indicating that ejection of the TTF molecules occurs upon oxidation, and establishing that $\mathbf{MS}^{4+}$ itself is not a good host to sustain the formation of TTF radical dimers in a supramolecular context. As in the case of traditional donor−acceptor bistable [2]-catenanes,[3b,6a] generation of the $TTF^{+\bullet}$ radical cation forces these species to leave the cavity of the MS^{4+} ring; the Coulombic repulsion between the charged $TTF^{+\bullet}$ unit and the tetracationic cyclophane is greater than the stability of TTF mixed-valence dimer, $(TTF)_2^{+\bullet}$. We then investigated the switching behaviors of two [3]catenanes $\mathbf{1}^{4+}$ and $\mathbf{2}^{4+}$ in which the TTF units are held in place by means of a couple of mechanical bonds. The oxidative region of the cyclic voltammogram of $\mathbf{1}^{4+}$ displays three oxidation peaks, which indicate one- (+400 mV), one- (+600 mV), and two-electron (+800 mV) processes, respectively. Corresponding re-reductions are observed indicating complete reversibility of these processes. In the case of $\mathbf{2}^{4+}$, in which the DNP units have been replaced with butadiyne subunits, the oxidative region shows four one-electron processes occurring with peak potentials at +410, +660, +1320, +1470 mV. In both [3]catenanes, the first two oxidation events correspond to the formation of the mixed-valence dimer and the radical-cation dimer, respectively. Unlike $\mathbf{1}^{4+}$, the third and the fourth oxidation peaks of $\mathbf{2}^{4+}$ are shifted to significantly higher potentials, indicating the formation of a stable $(TTF^{+\bullet})_2$ dimer. It follows that the distribution of the $(TTF^{+\bullet})_2$ dimer can be fine-tuned (Figure 4b) by varying the secondary recognition sites in mechanically interlocked molecules, such as in [3]catenanes, and also in a recently reported[12] [3]rotacatenane.

To rationalize the switching properties of the [3]catenanes, we propose (Figure 5) a different switching mechanism for each [3]catenane according to its secondary recognition sites. One-electron oxidation of the TTF units results in the formation of the mixed-valence dimer $(TTF)_2^{+\bullet}$ in both [3]catenanes—namely, $\mathbf{1}^{5+}$ and $\mathbf{2}^{5+}$—followed by subsequent one-electron oxidation to form the corresponding radical-cation dimers $(TTF^{+\bullet})_2$, labeled as $\mathbf{1}^{6+}$ and $\mathbf{2}^{6+}$. Interestingly, the final oxidation potential of $\mathbf{1}^{6+}$ at +800 mV, where the second oxidation of each TTF unit occurs, does not exhibit a significant shift when compared to the second oxidation potentials of the control compounds shown in Figure 4. We attribute this result to the presence of the DNP recognition sites which compete with the radical-cation dimer $(TTF^{+\bullet})_2$ for occupancy inside the cavity of MS^{4+}. We propose therefore that the final two-electron oxidation of $\mathbf{1}^{6+}$ is a result of the formation of an equilibrium between the radical-cation dimer state, $\mathbf{1}_{in}^{6+}$, and the newly formed $\mathbf{1}_{out}^{6+}$ state, where both $TTF^{+\bullet}$ units leave the cavity of the tetracationic cyclophane by dint of circumrotation, thus allowing the second oxidation of the $TTF^{+\bullet}$ units to occur at somewhat lower oxidation potentials, reflecting a situation which is typical of a "free" TTF unit. We hypothesize that, at slower scan rates, newly generated $\mathbf{1}_{in}^{6+}$ has enough time to establish an equilibrium between itself and the $\mathbf{1}_{out}^{6+}$ state and, as the oxidation of the $TTF^{+\bullet}$ unit located outside the cyclophane occurs, the equilibrium shifts toward the $\mathbf{1}_{out}^{6+}$ state resulting in an overall two-electron process at +800 mV. This result can also be rationalized by the fact that, in the UV−vis−NIR spectra (Figure 3), the intensity of the radical-cation dimer absorption peak at 800 nm corresponding to $\mathbf{1}_{in}^{6+}$ state is significantly lower than that observed for $\mathbf{2}^{6+}$ state. This hypothesis is further supported by the presence of a significant positive shift in the third oxidation peak of $\mathbf{2}^{4+}$, in which the DNP units are replaced with butadiyne subunits that have little or no affinity for the tetracationic cyclophane. Since little or no energetic stabilization is afforded by the occupancy of the butadiyne units in the cyclophane, the equilibrium greatly favors the retention of the TTF radical-cation dimer within the cavity of MS^{4+}, despite the inherently repulsive electrostatic interactions between the charged radical cations and the tetracationic cyclophane. The formation of the $\mathbf{2}^{7+}$ state occurs upon the oxidative generation of one TTF^{2+} dication, which is ejected from the cavity of the tetracationic cyclophane, causing the circumrotation of one of the crown ethers such that its butadiyne unit occupies the cavity of the cyclophane. Therefore, the $TTF^{+\bullet}$ radical-cation associated with the other crown ether can form[11] an intermediate dimer with the butadiyne unit, establishing an interaction within the

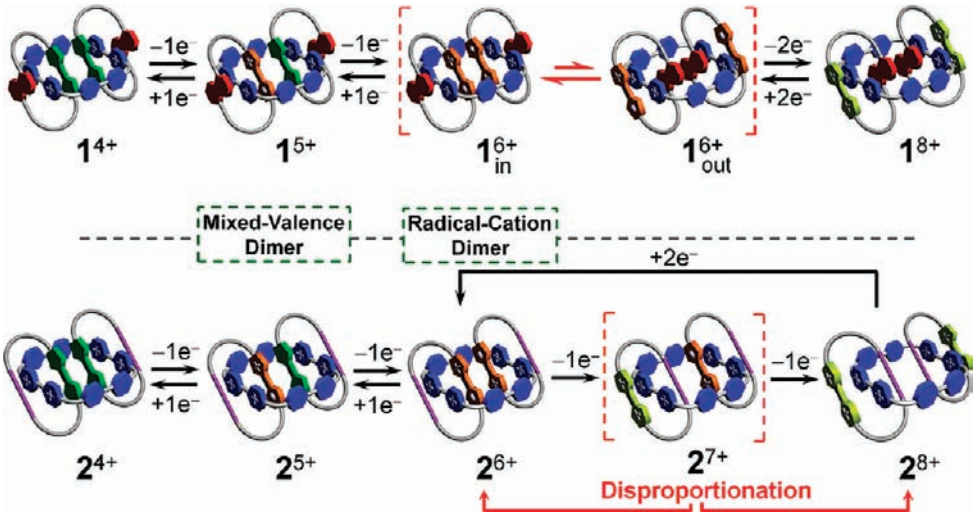

Figure 5. Proposed redox-controlled switching mechanisms taking place within the two [3]catenanes. In both cases, the first two one-electron processes lead to the formation of the mixed-valence dimer states ($\mathbf{1}^{5+}$ and $\mathbf{2}^{5+}$) in the first event, and then the radical-cation dimer states ($\mathbf{1}_{in}^{6+}$ and $\mathbf{2}^{6+}$) subsequently. We propose the formation of an equilibrium state between $\mathbf{1}_{in}^{6+}$ and $\mathbf{1}_{out}^{6+}$ in which the DNP units share the occupation of the cavity of the tetracationic cyclophane. The final two-electron oxidation to $\mathbf{1}^{8+}$ is believed to proceed from the $\mathbf{1}_{out}^{6+}$ state. The formation of intermediate $\mathbf{2}^{7+}$ results in disproportionation to more stable states $\mathbf{2}^{6+}$ and $\mathbf{2}^{8+}$.

dx.doi.org/10.1021/ja110584c |*J. Am. Chem. Soc.* 2011, 133, 4538–4547

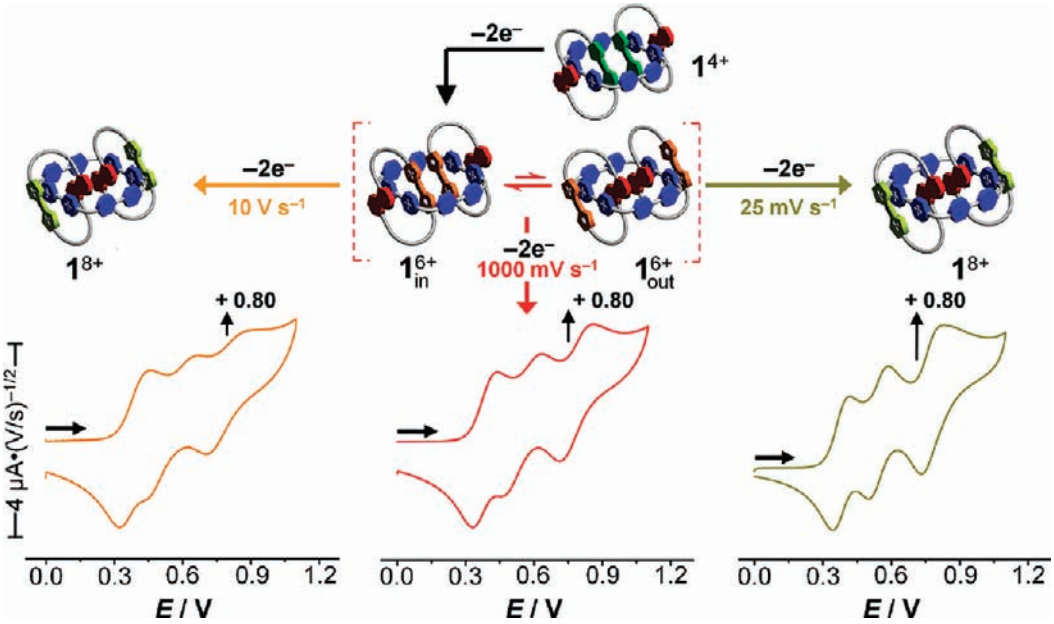

Figure 6. Variable scan rate CV measurements of $\mathbf{1}^{4+}$ in MeCN at room temperature. At fast scan rates (10 V s^{-1}, left), a decrease in the oxidation process at +800 mV potential is observed, since there is not enough time for the equilibration to occur. At intermediate scan rates (1 V s^{-1}, middle), an increase in the oxidation process at +800 mV was observed. At relatively slow scan rates (25 mV s^{-1}, right), we have driven the equilibrium in such a way that nearly all of the $\mathbf{1}_{out}{}^{6+}$ undergoes oxidation, resulting in an oxidation-driven shift in the equilibrium process to form $\mathbf{1}_{out}{}^{6+}$, which corresponds ultimately to a two-electron process.

cavity of MS^{4+}. The final oxidation of $\mathbf{2}^{7+}$ results in the removal of the second TTF^{2+} dication from the cavity of the tetracationic cyclophane, forming the fully oxidized $\mathbf{2}^{8+}$ state in which both butadiyne units are located inside the cavity. The re-reductions of both $\mathbf{1}^{8+}$ and $\mathbf{2}^{8+}$ occur as two-electron processes at +710 mV, proving that the fully oxidized TTF^{2+} units leave the cavity of the cyclophane and are re-reduced to form TTF radical cations while residing outside the cyclophane. Subsequent re-reductions of the $\mathbf{1}^{6+}$ and $\mathbf{2}^{6+}$ states at +490 mV supports the reformation of radical-cation dimers, despite the presence of charge−charge repulsions and demonstrates the full reversibility of the oxidation processes. The reduction cycles of the two [3]catenanes reveal two reduction peaks associated with $BIPY^{2+}$, observed at −540 and −890 mV and corresponding, in turn, to two two-electron processes. The return anodic scan displays the corresponding re-oxidation peaks, indicating the reversibility of these processes for both $\mathbf{1}^{4+}$ and $\mathbf{2}^{4+}$.

To provide further evidence for the existence of the equilibrium initiated after the two-electron oxidation of $\mathbf{1}^{4+}$ to $\mathbf{1}^{6+}$, wherein the $TTF^{+\bullet}$ units can reside inside ($\mathbf{1}_{in}{}^{6+}$) or outside ($\mathbf{1}_{out}{}^{6+}$) the cavity, we performed (Figure 6) variable scan-rate CV experiments on $\mathbf{1}^{4+}$. At 10 V s^{-1}, we can only detect a small peak at +800 mV, an observation which indicates total equilibration has not yet occurred. Attempts to measure the oxidation of the $TTF^{+\bullet}$ units remaining inside the cavity, i.e., as part of $\mathbf{1}_{in}{}^{6+}$, were hindered by the irreversible oxidation of the DNP groups at higher potentials. On slowing the scan rate down to +1000 mV s^{-1}, it is clear that the peak at +800 mV increases in intensity, reflecting an approximately one-electron process, after peak integration. At 25 mV s^{-1}, a two-electron process is apparent, suggesting that the driving of the equilibrium toward the $\mathbf{1}_{out}{}^{6+}$ state has occurred, thus supporting the proposed switching mechanism (Figure 5).

Further spectroscopic evidence for the formation of the radical dimers of tetrathiafulvalene was provided (Figure 7) by CW EPR measurements. The EPR spectra for both [3]catenanes $\mathbf{1}^{4+}$ and $\mathbf{2}^{4+}$ were recorded in MeCN (0.3 mM) at 295 K on titration with the oxidant $Fe(ClO_4)_3$ to generate the oxidized states. Formation of the mixed-valence states, $\mathbf{1}^{5+}$ and $\mathbf{2}^{5+}$, was observed upon addition of 1.0 equiv of oxidant to each solution. It is important to note that the stability of the mixed-valence state $(TTF)_2{}^{+\bullet}$ in $\mathbf{1}^{5+}$ is not affected by the presence of secondary binding, proving that the stability of the mixed-valence dimer $(TTF)_2{}^{+\bullet}$ can overcome the charge−charge destabilization. Upon addition of 2.0 equiv of the oxidant, a remarkable difference between the EPR spectra of $\mathbf{1}^{6+}$ and $\mathbf{2}^{6+}$ was observed. In the case of $\mathbf{2}^{6+}$, attenuation of the EPR signal occurred as a result of the strong spin-coupling between the $TTF^{+\bullet}$ moieties, forming an EPR-silent species. Only a slight decrease in the EPR signal intensity of $\mathbf{1}^{6+}$ was observed, suggesting[20] the presence of the EPR-active species $\mathbf{1}_{out}{}^{6+}$ in the solution. In agreement with the CV and UV/vis experiments, once the TTF radical-cation dimer state $\mathbf{1}_{in}{}^{6+}$ is generated, the formation of an equilibrium is observed between the $\mathbf{1}_{in}{}^{6+}$ and $\mathbf{1}_{out}{}^{6+}$. Unlike the mixed-valence state $\mathbf{1}^{5+}$, the stability of the radical-cation dimer $(TTF^{+\bullet})_2$ in $\mathbf{1}^{6+}$ cannot completely overcome the destabilizing electrostatic interactions, resulting partially in the circumrotation of the ring component to form the $\mathbf{1}_{out}{}^{6+}$ state in which the two DNP units are located within the cavity of the cyclophane. Moreover, the equilibrium distribution of both the $\mathbf{1}_{in}{}^{6+}$ and $\mathbf{1}_{out}{}^{6+}$ states can be determined[21] based on the EPR signal intensities. The data indicate that the equilibrium distribution is approximately 60:40 in favor of $\mathbf{1}_{in}{}^{6+}$ state. Further additions of the oxidant in small portions up until 4.0 equiv resulted in a gradual decrease in the signal intensity, which eventually disappeared as a result of the formation of the EPR silent $\mathbf{1}^{8+}$ state. Although addition of 3.0 equiv oxidant to $\mathbf{2}^{4+}$ should, in theory, form the $\mathbf{2}^{7+}$ state, we did not observe the re-emergence of an EPR signal upon addition of the third equivalent of oxidant.

dx.doi.org/10.1021/ja110584c |*J. Am. Chem. Soc.* 2011, 133, 4538–4547

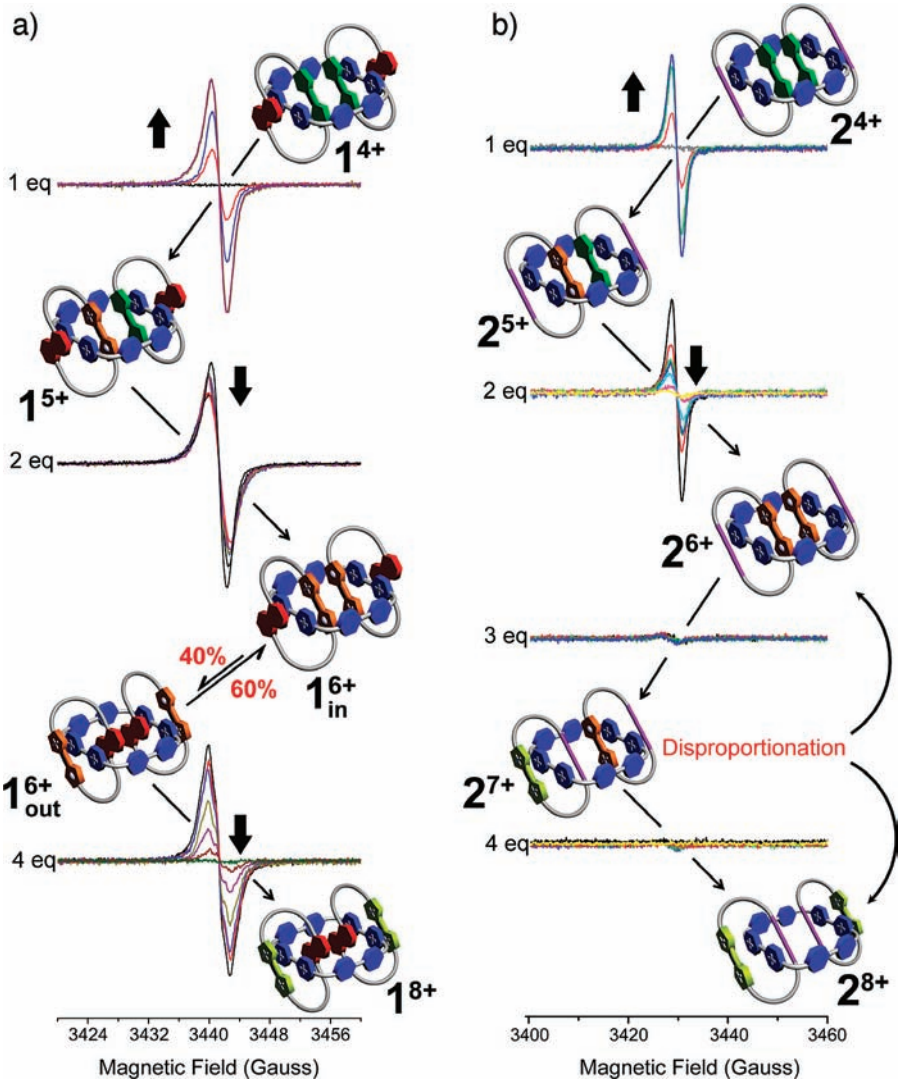

Figure 7. CW EPR spectra of (a) $\mathbf{1}^{4+}$ and (b) $\mathbf{2}^{4+}$ (0.3 mM in MeCN, 295 K) recorded upon stepwise oxidation of the two [3]catenanes with $Fe(ClO_4)_3$. Upon addition of 1.0 equiv of the oxidant in the case of both [3]catenanes, the stable mixed-valence states $\mathbf{1}^{5+}$ and $\mathbf{2}^{5+}$ are formed. The addition of 2.0 equiv of the oxidant results in the attenuation of the radical signal in the case of $\mathbf{2}^{6+}$, whereas a slight decrease in the EPR signal intensity of $\mathbf{1}^{6+}$ is observed, suggesting the presence of the EPR-active species $\mathbf{1}_{out}{}^{6+}$ as a consequence of the formation of an equilibrium with $\mathbf{1}_{in}{}^{6+}$. In the case of $\mathbf{2}^{7+}$, the absence of any EPR activity suggests the disproportionation of $\mathbf{2}^{7+}$ to the $\mathbf{2}^{6+}$ and $\mathbf{2}^{8+}$ states. Further oxidation of both [3]catenanes, up until 4.0 equiv of oxidant, results in the formation of the fully oxidized states $\mathbf{1}^{8+}$ and $\mathbf{2}^{8+}$.

Hence, we propose that the transient $\mathbf{2}^{7+}$ species disproportionates, to form the EPR-inactive $\mathbf{2}^{6+}$ and $\mathbf{2}^{8+}$ species.[22] This mechanism is also supported by CV experiments where the formation of $\mathbf{2}^{7+}$ is found to be irreversible. Further addition of the oxidant did not cause any change in the spectrum as a result of the formation of the $\mathbf{2}^{8+}$state.

The stability afforded to the TTF dimers by encapsulation within the confines of the tetracationic cyclophane makes it possible to study their solid-state structures (Figure 8) by single crystal X-ray diffraction analysis. Simply by titrating the appropriate number of equivalents of $Fe(ClO_4)_3$—as a solution in MeCN—into $MeNO_2$ or MeCN solutions of the [3]catenanes, the mixed-valence states $\mathbf{1}^{5+}$ and $\mathbf{2}^{5+}$, and the radical-cation dimer states $\mathbf{1}^{6+}$ and $\mathbf{2}^{6+}$, can be accessed. Subsequent vapor diffusion of Et_2O into the catenane solutions in MeCN or $MeNO_2$ at 0 °C yielded single crystals[23] of $\mathbf{1}^{5+}$, $\mathbf{2}^{5+}$, and $\mathbf{2}^{6+}$ suitable for X-ray analysis. The fact that we could crystallize these oxidized states, which represent the binding of mono- and dicationic moieties by the tetracationic cyclophane, attests to the relative stabilities of these radical dimers within the mechanically interlocked structure.

The difference in interaction between the TTF units in the two dimers is evidenced[24] by (i) the distance between the two TTF dimers, (ii) the angle of offset of the TTF units, and (iii) the vertical offset of the TTF units. These structural changes are evident when comparing the solid-state structures of the ground state of $\mathbf{1}^{4+}$ and its mixed valence state, $\mathbf{1}^{5+}$ — the TTF units of $\mathbf{1}^{4+}$ are separated by 3.68 Å and offset by 0.8 Å and 16.7°, whereas in the case of $\mathbf{1}^{5+}$, the interplanar distance (Figure 8a) is 3.42 Å with a negligible angular offset of 0.3° but a pronounced vertical offset of 1.4 Å. This plane-to-plane TTF···TTF distance is shorter than that expected for a mixed-valence dimer,[7h,8b,25] given the fact that their interaction is presumably weakened by the vertical offset. The average distance, however, between like

dx.doi.org/10.1021/ja110584c |*J. Am. Chem. Soc.* 2011, 133, 4538–4547

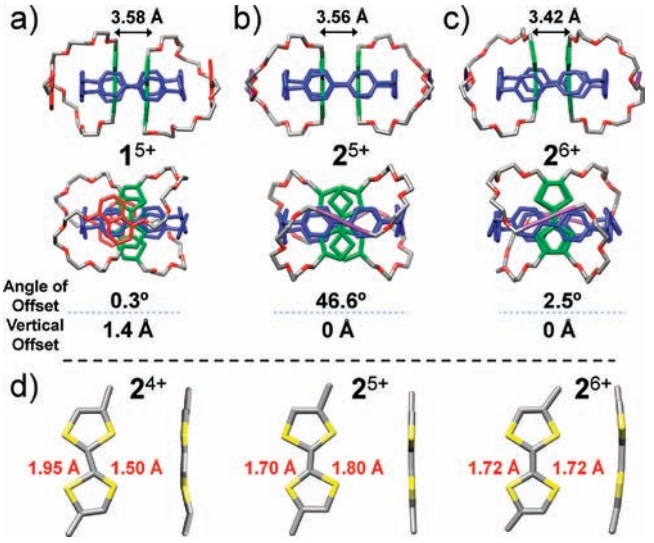

Figure 8. Crystal structures of the mixed-valence states (a) $\mathbf{1}^{5+}$ and (b) $\mathbf{2}^{5+}$, and the radical-cation dimer state (c) $\mathbf{2}^{6+}$. (a) Upon oxidation of the TTF unit, the interplanar distance between two TTF units shrinks to 3.58 Å from being 3.68 Å (see Figure 2) in the ground state $\mathbf{1}^{4+}$. (b) Similarly, in the case of $\mathbf{2}^{5+}$, formation of the mixed-valence state brings the interplanar distance between the TTF units down to 3.56 Å. (c) The radical-cation dimer state $\mathbf{2}^{6+}$ experiences almost perfect overlapping of the TTF units with an interplanar distance of 3.42 Å. The angle of offset is defined by the relative orientations of the C═C double bonds in the TTF units: when these bonds are eclipsed the angle is 0°. The vertical offset is the measure of offset between the planes of the TTF units: when these TTF units are in register, the vertical offset value is 0 Å. (d) The changes in C−S bond lengths, between the central C═C double bond and the sulfur atom, upon oxidation of the TTF unit in $\mathbf{2}^{4+}$.

atoms of the TTF dimer is 3.58 Å — a value closer to that expected of a mixed-valence dimer. The crystal structure of the ground state of $\mathbf{2}^{4+}$ has the TTF units arranged in a slipped-stack manner, separated by 3.68 Å, whereas the solid-state structure (Figure 8b) of the mixed-valence state, $\mathbf{2}^{5+}$ brings the TTF units closer together, at a distance of 3.56 Å, with no vertical offset but subtending an angle of 46.6° with respect to the central C═C bonds of each TTF unit. Finally, the crystal structure (Figure 8c) of $\mathbf{2}^{6+}$, the radical-cation dimer, has its TTF units overlapping almost perfectly, with no vertical offset and an angular offset of only 2.5°. The interplanar spacing is 3.42 Å, with the closest contacts between the C atoms of the C═C bonds as low as 3.33 Å. The TTF···TTF spacings in both the mixed-valence state and the radical-cation dimer are commensurate with values reported[25] for structures previously in the literature. When analyzing the solid-state structures of these TTF-containing compounds, it is important to appreciate the significance of the unique environment the TTF moieties experience in the mechanically interlocked context of the [3]catenanes. There is a whole gamut of noncovalent bonding interactions present in these molecules — namely, [C−H···O] and [$\pi\cdots\pi$] stacking interactions, as well as [C−H···π] contacts — which dictate many features of the structures, and their influence simply has to be felt by the TTF units themselves. This point is reflected in the significant distortion from planarity and uniformity of the TTF units in the ground state structures $\mathbf{1}^{4+}$ and $\mathbf{2}^{4+}$. The TTF-containing macrocycles which constitute $\mathbf{2}^{4+}$ are shorter in terms of number of linking atoms — 28 in contrast to 32 — when compared to those of $\mathbf{1}^{4+}$, and as such, the TTF units in $\mathbf{2}^{4+}$ experience considerable distortion in the ground state when there is clearly little or no interaction between the TTF units. The C−S bond lengths (Figure 8d) between the central C═C double bond and the sulfur atoms vary from 1.45 to 1.90 Å, whereas the C═C−S bond angles[26] are far from 120°—see the Supporting Information for the detailed analysis of the bond lengths and angles, Table S1 and S2. On removal of one electron to form the TTF mixed-valence dimer $\mathbf{2}^{5+}$, changes in geometry are noticeable; there exists quite a lot of deviation from uniformity in bond lengths and angles (less so than in the ground state), whereas the TTF units are almost planar. These changes in bond lengths and angles may occur on account of the partial aromatic character generated in one TTF unit upon one-electron oxidation, whereas the planarity may be as a result of interaction between the TTF units in the mixed-valence dimer. It should be noted that both TTF units display very similar geometries, indicating the interacting and delocalized nature of the single radical in the dimer. Further oxidation to the radical cation dimer in $\mathbf{2}^{6+}$ once again affects the geometry of the TTF units. Both molecules now have partial aromatic character, and the bond lengths and angles are uniform. Interestingly, the TTF molecules are not entirely planar although each five-membered ring component itself is almost perfectly planar, the C atoms of the C═C double bonds appear to be drawn closer to each other[25,27] whereas the planes of the five-membered rings point away from the dimer. This relative geometry may be indicative of the beginnings of radical overlap to form a partial covalent bond between the central C atoms of the two TTF units, a phenomenon which has been predicted[11,27] by theory to have 20% covalent character in a cyclobutane-like arrangement. In addition, we have also observed (see the Supporting Information, Figure S1) short [C−H···O] and [C−H···F] contacts between the oxidized TTF units and the surrounding ClO_4^- and PF_6^- counterions which could possibly contribute to the stabilization of the TTF radical dimers in $\mathbf{1}^{5+}$, $\mathbf{2}^{5+}$, and $\mathbf{2}^{6+}$ in the solid-state.

Previously, we have investigated[11] the switching mechanism of $\mathbf{2}^{4+}$ using density functional theory (DFT). The switching mechanism of $\mathbf{1}^{4+}$ has now also been investigated using the same theoretical/computational approach/analysis. We have already shown[28] that the M06-suite[29] of density functionals is a good choice for the description of mechanically interlocked molecules of similar constitutions. Using the X-ray structural data as a starting point, structures for $\mathbf{1}^{4+}/\mathbf{1}^{5+}/\mathbf{1}^{6+}/\mathbf{1}^{7+}/\mathbf{1}^{8+}$ were generated in three different co-conformations named according to the relative position of the TTF units: in−in, in−out, and out−out. All structures were then minimized in the gas phase using the M06 functional and 6-31G* basis set. A comparison of the calculated and X-ray structures for $\mathbf{1}^{n+}$ (where $\mathbf{n} = 4$−8) shows that our choice of computational approach is able to reproduce the medium-range interactions responsible for most of the key recognition elements in the structure. For example, the interplanar separation between the inside TTF units and the plane of the $BIPY^{2+}$ units is around 3.4 Å (experimental range from 3.33 to 3.58 Å), whereas the distance between TTF units within the cavity of tetracationic cyclophane is around 3.6 Å compared with the experimental value of 3.7 Å.

The relative solvation-corrected energetic (M06/6-311++G** level) landscape (Table 1) exhibits a profile consistent with the electrochemical fingerprint observed for the switching process. It is evident that, by comparison with $\mathbf{2}^{n+}$, the recognition of the DNP units by the tetracationic cyclophane

dx.doi.org/10.1021/ja110584c | J. Am. Chem. Soc. 2011, 133, 4538–4547

Table 1. Calculated Relative Energetic Landscape for the in−in, in−out, and out−out Co-conformations. Energies are Solvent-Corrected Electronic Energies at the M06/6-311++G** Level in kcal/mol[a]

co-conformations	1^{4+}	1^{5+}	1^{6+}	1^{7+}	1^{8+}
in−in	0.0 (0.0)	0.0 (0.0)	0.0 (0.0)	4.9 (44.1)	52.2 (224.3)
in−out	16.3 (35.2)	16.5 (38.8)	36.1 (53.0)	4.8 (45.7)	35.8 (190.4)
out−out	20.6 (53.1)	10.3 (27.9)	1.0 (25.9)	0.0 (0.0)	0.0 (0.0)

[a] Values in parentheses are gas-phase energies.

stabilizes the out−out co-conformation, especially in 1^{6+} where this geometry becomes competitive with the binding of the radical-cation dimer $(TTF^{+\bullet})_2$. In 1^{7+} and 1^{8+}, the out−out co-conformation is more stable than the in−in one. Notably, the gas-phase relative stabilities for the different co-conformations show a similar trend. The unscreened charge repulsion dominates, however, and thus the magnitude of the differences tends to be larger. The screening of charge by the solvent (dielectric) in highly charged mechanically interlocked molecules reduces quite significantly the electrostatic repulsive interactions. More importantly, the variation in solvation energy for the different co-conformations plays a key role in determining their relative stabilities. Even though this trend may be more apparent in aqueous environments,[30] in polar organic solvents such as MeCN, it is of considerable importance. Increased solvation stabilization is present in co-conformations where the charge is more accessible to solvent molecules, such as for those co-conformations where the oxidized TTF units are not encircled by the tetracationic cyclophane. This scenario also allows for more interaction of the solvent with the $\mathbf{1}_{out}^{6+}$ state. This effect is demonstrated by the differences in the relative gas-phase and solvent-corrected energetic landscapes. For example, in 1^{6+}, the in−in co-conformation is predicted to be more stable than the out−out one by ∼26 kcal/mol in the gas phase, but only by 1 kcal/mol in MeCN — a very small difference which explains the equilibrium observed in solution between the two co-conformations. This apparent discrepancy is a consequence of the marked differences in the solvation energies of the two co-conformations. The in−in co-conformation has most of the positive charge focused on the tetracationic cyclophane and the encircled oxidized TTF groups, while the out−out co-conformation has the tetracationic cyclophane more available for solvation and the oxidized TTF units are also able to be independently solvated. The interaction of solvent, and indeed the counterions, with the charged TTF dimers has previously been predicted[7h,27] to be a significant factor in the stabilization of the dimers in solution. In the unique environment of mechanically interlocked [3]catenanes; however, accessibility of the dimers to solvent is somewhat limited and we cannot rule out the possibility that this solvation aids the stabilization of these species.

CONCLUSIONS

The mechanical stabilization of TTF radical dimers in [3]catenanes, namely, molecular flasks, under ambient conditions has been demonstrated. The mechanically interlocked nature of the [3]catenanes allows us to study intermolecular interactions between the TTF radical dimers in a molecule. It has also been shown that the stabilities of the TTF radical-cation dimers can be fine-tuned by varying the secondary binding motifs in [3]catenanes. These findings have led to the fundamental understanding of the intermolecular interactions between TTF radical dimers and also represent the introduction of radical binding as a recognition motif to drive switching in mechanically interlocked molecules.[31] The results could contribute in the fullness of time to the development of molecular electronic devices based on tetrathiafulvalene units.

EXPERIMENTAL SECTION

General Methods. All reagents were purchased from commercial suppliers (Aldrich or Fisher) and used without further purification. $\mathbf{1}\cdot 4PF_6$[11], $\mathbf{2}\cdot 4PF_6$[11], and $\mathbf{MS}\cdot 4PF_6$[13] were prepared following procedures reported in the literature. UV−vis−NIR absorbance spectra were recorded using a Perkin-Elmer LAMBDA 1050 double beam, double monochromator, ratio-recording spectrometer. EPR Measurements at X-band (9.5 GHz) were made using a Bruker Elexsys E580. The EPR spectrometer was equipped with a variable Q dielectric resonator (ER-4118X-MD5-W1). Steady-state CW EPR spectra were measured using 0.2−2 mW microwave power and 0.01−0.05 mT field modulation at 100 kHz, with a time constant of 5.12 ms and a conversion time of 40.96 ms. Cyclic voltammetry experiments were performed on a Gamry Reference 600 potentiostat interfaced to a PC, using a glassy carbon working electrode (0.018 cm^2, Cypress system) in argon-purged MeCN solutions at room temperature. The electrode surface was polished routinely with 0.05 μm alumina/water slurry on a felt surface immediately before use. The counter electrode was a Pt coil and the reference electrode was a standard Ag/AgCl electrode. The concentrations of the samples were 1 mM in 100 mM electrolyte solution ($TBAPF_6$ in MeCN).

Computational Methods. Calculations were performed on all systems using density functional theory (DFT) with the M06 functional, as implemented[32] in Jaguar 7.6r110. Starting with a structure from the crystallographic data, we optimized the geometry using the 6-31G* basis set in the gas phase. The relative electronic solvation-corrected energetic landscape was calculated at the M06/6-311++G** level of theory.

ASSOCIATED CONTENT

Supporting Information. Detailed X-ray crystallographic analysis data (CIF). This material is available free of charge via the Internet at http://pubs.acs.org.

AUTHOR INFORMATION

Corresponding Author
stoddart@northwestern.edu

ACKNOWLEDGMENT

We (J.F.S. and co-workers) acknowledge support from the Air Force Office of Scientific Research (AFSOR) under the Multidisciplinary Research Program of the University Research Initiative (MURI) Award FA9550-07-1-0534 on "Bioinspired Supramolecular Enzymatic Systems" and the National Science Foundation (NSF) under the auspices of Award CHE-0924620. J.F.S. and W.A.G. acknowledge support by the Microelectronics Advanced Research Corporation (MARCO) and its Focus

Center Research Program (FCRP) on Functional Engineered NanoArchitectonics (FENA). Computational facilities were funded by grants from ARO−DURIP and ONR-DURIP. M.R. W. acknowledges support by the National Science Foundation (NSF) under Grant CHE-1012378. R.C. was supported as part of the ANSER Center, an Energy Frontier Research Center (EPFRC) funded by the U.S. Department of Energy (DOE), Office of Science, Office of Basic Energy Sciences, under Award No. DE-SC0001059. D.B., E.T., and W.A.C acknowledge support from the U.S. Department of Energy (DOE), Office of Science, Office of Basic Energy Sciences under Award No. DE-PS-08GO98004P. G.B. was supported as part of the Non-Equilibrium Research Center (NERC), which is an Energy Fronties Research Center (EFRC) funded by the U.S. Department of Energy (DOE), Office of Science, Office of Basic Energy Sciences under Award No. DE-SC0000989. M.T.C. thanks the Link Foundation for a fellowship. G.B. thanks the International Center for Diffraction Data for the award of a 2011 Ludo Frevel Crystallography Scholarship. J.M.S. and A.C.F. acknowledge the National Science Foundation (NSF) for a Graduate Research Fellowship and J.M.S. acknowledges Northwestern University for a Presidential Fellowship.

■ REFERENCES

(1) (a) Bryce, M. R. *J. Mater. Chem.* **2000**, *10*, 589–598. (b) Nielsen, M. B.; Lomholt, C.; Becher, J. *Chem. Soc. Rev.* **2000**, *29*, 153–164. (c) Segura, J. L.; Martín, N. *Angew. Chem., Int. Ed.* **2001**, *40*, 1372–1409. (d) Inagi, S.; Naka, K.; Chujo, Y. *J. Mater. Chem.* **2007**, *17*, 4122–4135. (e) Martin, N.; Sanchez, L.; Herranz, M. A.; Illescas, B.; Guldi, D. M. *Acc. Chem. Res.* **2007**, *40*, 1015–1024. (f) Canevet, D.; Salle, M.; Zhang, G. X.; Zhang, D. Q.; Zhu, D. B. *Chem. Commun.* **2009**, 2245–2269. (g) Klajn, R.; Stoddart, J. F.; Grzybowski, B. A. *Chem. Soc. Rev.* **2010**, *39*, 2203–2237.

(2) (a) Becher, J.; Lau, J.; Leriche, P.; Mork, P.; Svenstrup, N. *J. Chem. Soc., Chem. Commun.* **1994**, 2715–2716. (b) Garin, J.; Orduna, J.; Uriel, S.; Moore, A. J.; Bryce, M. R.; Wegener, S.; Yufit, D. S.; Howard, J. A. K. *Synthesis* **1994**, 489–493. (c) Moore, A. J.; Bryce, M. R. *Synthesis* **1997**, 407–409. (d) Simonsen, K. B.; Becher, J. *Synlett* **1997**, 1211–1220. (e) Jeppesen, J. O.; Nielsen, M. B.; Becher, J. *Chem. Rev.* **2004**, *104*, 5115–5131.

(3) (a) Li, Z. T.; Stein, P. C.; Becher, J.; Jensen, D.; Mork, P.; Svenstrup, N. *Chem.—Eur. J.* **1996**, *2*, 624–633. (b) Asakawa, M.; Ashton, P. R.; Balzani, V.; Credi, A.; Hamers, C.; Mattersteig, G.; Montalti, M.; Shipway, A. N.; Spencer, N.; Stoddart, J. F.; Tolley, M. S.; Venturi, M.; White, A. J. P.; Williams, D. J. *Angew. Chem., Int. Ed.* **1998**, *37*, 333–337. (c) Kang, S. S.; Vignon, S. A.; Tseng, H.-R.; Stoddart, J. F. *Chem.—Eur. J.* **2004**, *10*, 2555–2564. (d) Liu, Y.; Bruneau, A.; He, J. M.; Abliz, Z. *Org. Lett.* **2008**, *10*, 765–768. (e) Cao, D.; Amelia, M.; Klivansky, L. M.; Koshkakaryan, G.; Khan, S. I.; Semeraro, M.; Silvi, S.; Venturi, M.; Credi, A.; Liu, Y. *J. Am. Chem. Soc.* **2010**, *132*, 1110–1122. (f) Wang, C.; Olson, M. A.; Fang, L.; Benítez, D.; Tkatchouk, E.; Basu, S.; Basuray, A. N.; Zhang, D. Q.; Zhu, D. B.; Goddard, W. A.; Stoddart, J. F. *Proc. Natl. Acad. Sci. U.S.A.* **2010**, *107*, 13991–13996.

(4) Wudl, F.; Wobschal., D; Hufnagel, E. J. *J. Am. Chem. Soc.* **1972**, *94*, 670–672.

(5) Ferraris, J.; Cowan, D. O.; Walatka, V.; Perlstein, J. H. *J. Am. Chem. Soc.* **1973**, *95*, 948–949.

(6) (a) Collier, C. P.; Mattersteig, G.; Wong, E. W.; Luo, Y.; Beverly, K.; Sampaio, J.; Raymo, F. M.; Stoddart, J. F.; Heath, J. R. *Science* **2000**, *289*, 1172–1175. (b) Flood, A. H.; Stoddart, J. F.; Steuerman, D. W.; Heath, J. R. *Science* **2004**, *306*, 2055–2056. (c) Heath, J. R.; Stoddart, J. F.; Williams, R. S. *Science* **2004**, *303*, 1136–1137. (d) Green, J. E.; Choi, J. W.; Boukai, A.; Bunimovich, Y.; Johnston-Halperin, E.; DeIonno, E.; Luo, Y.; Sheriff, B. A.; Xu, K.; Shin, Y. S.; Tseng, H.-R.; Stoddart, J. F.; Heath, J. R. *Nature* **2007**, *445*, 414–417. (e) Heath, J. R. *Ann. Rev. Mater. Res.* **2009**, *39*, 1–23.(f) van der Molen, S. J.; Liljeroth, P. *J. Phys.: Condens. Matter* **2010**, *22*, 133001; (g) Zhang, W.; DeIonno, E.; Dichtel, W. R.; Fang, L.; Trabolsi, A.; Olsen, J.-C.; Benítez, D.; Heath, J. R.; Stoddart, J. F. *J. Mater. Chem.* **2011**, *21*, 1487−1495.

(7) (a) Yakushi, K.; Nishimura, S.; Sugano, T.; Kuroda, H.; Ikemoto, I. *Acta Crystallogr. B* **1980**, *36*, 358–363. (b) Kathirgamanathan, P.; Mazid, M. A.; Rosseinsky, D. R. *J. Chem. Soc., Perkin Trans. 2* **1982**, 593–596. (c) Kondo, K.; Matsubayashi, G.; Tanaka, T.; Yoshioka, H.; Nakatsu, K. *J. Chem. Soc., Dalton Trans.* **1984**, 379–384. (d) Pyrka, G. J.; Fernando, Q.; Inoue, M. B.; Inoue, M. *Inorg. Chim. Acta* **1989**, *156*, 257–264. (e) Umeya, M.; Kawata, S.; Matsuzaka, H.; Kitagawa, S.; Nishikawa, H.; Kikuchi, K.; Ikemoto, I. *J. Mater. Chem.* **1998**, *8*, 295–300. (f) Spanggaard, H.; Prehn, J.; Nielsen, M. B.; Levillain, E.; Allain, M.; Becher, J. *J. Am. Chem. Soc.* **2000**, *122*, 9486–9494. (g) Schiccheri, N.; Meneghetti, M. *J. Phys. Chem. A* **2005**, *109*, 4643–4645. (h) Garcia-Yoldi, I.; Miller, J. S.; Novoa, J. J. *J. Phys. Chem. A* **2009**, *113*, 484–492. (i) Tanaka, K.; Kunita, T.; Ishiguro, F.; Naka, K.; Chujo, Y. *Langmuir* **2009**, *25*, 6929–6933.

(8) (a) Bozio, R.; Zanon, I.; Girlando, A.; Pecile, C. *J. Chem. Phys.* **1979**, *71*, 2282–2293. (b) Torrance, J. B.; Scott, B. A.; Welber, B.; Kaufman, F. B.; Seiden, P. E. *Phys. Rev. B* **1979**, *19*, 730–741. (c) Khodorkovsky, V.; Shapiro, L.; Krief, P.; Shames, A.; Mabon, G.; Gorgues, A.; Giffard, M. *Chem. Commun.* **2001**, 2736–2737. (d) Rosokha, S. V.; Kochi, J. K. *J. Am. Chem. Soc.* **2007**, *129*, 828–838.

(9) (a) Christensen, C. A.; Goldenberg, L. M.; Bryce, M. R.; Becher, J. *Chem. Commun.* **1998**, 509–510. (b) Lyskawa, J.; Sallé, M.; Balandier, J. Y.; Le Derf, F.; Levillain, E.; Allain, M.; Viel, P.; Palacin, S. *Chem. Commun.* **2006**, 2233–2235. (c) Aprahamian, I.; Olsen, J.-C.; Trabolsi, A.; Stoddart, J. F. *Chem.—Eur. J.* **2008**, *14*, 3889–3895.

(10) (a) Ziganshina, A. Y.; Ko, Y. H.; Jeon, W. S.; Kim, K. *Chem. Commun.* **2004**, 806–807. (b) Yoshizawa, M.; Kumazawa, K.; Fujita, M. *J. Am. Chem. Soc.* **2005**, *127*, 13456–13457. (c) Chiang, P.-T.; Chen, N.-C.; Lai, C.-C.; Chiu, S.-H. *Chem.—Eur. J.* **2008**, *14*, 6546–6552. (d) Saad, A.; Barriere, F.; Levillain, E.; Vanthuyne, N.; Jeannin, O.; Fourmigue, M. *Chem.—Eur. J.* **2010**, *16*, 8020–8028.

(11) Spruell, J. M.; et al. *Nature Chem.* **2010**, *2*, 870–879.

(12) Barin, G.; Coskun, A.; Friedman, D. C.; Olson, M. A.; Colvin, M. T.; Carmielli, R.; Dey, S. K.; Bozdemir, O. A.; Wasielewski, M. R.; Stoddart, J. F. *Chem.—Eur. J.* **2011**, *17*, 213–222.

(13) Asakawa, M.; Ashton, P. R.; Menzer, S.; Raymo, F. M.; Stoddart, J. F.; White, A. J. P.; Williams, D. J. *Chem.—Eur. J.* **1996**, *2*, 877–893.

(14) Odell, B.; Reddington, M. V.; Slawin, A. M. Z.; Spencer, N.; Stoddart, J. F.; Williams, D. J. *Angew. Chem., Int. Ed.* **1988**, *27*, 1547–1550.

(15) Olson, M. A.; Botros, Y. Y.; Stoddart, J. F. *Pure Appl. Chem.* **2010**, *82*, 1569–1574.

(16) Hunter, C. A. *J. Chem. Soc., Chem. Commun.* **1991**, 749–751.

(17) (a) Houk, K. N.; Menzer, S.; Newton, S. P.; Raymo, F. M.; Stoddart, J. F.; Williams, D. J. *J. Am. Chem. Soc.* **1999**, *121*, 1479–1487. (b) Raymo, F. M.; Bartberger, M. D.; Houk, K. N.; Stoddart, J. F. *J. Am. Chem. Soc.* **2001**, *123*, 9264–9267.

(18) (a) Miljanić, O. Š.; Dichtel, W. R.; Khan, S. I.; Mortezaei, S.; Heath, J. R.; Stoddart, J. F. *J. Am. Chem. Soc.* **2007**, *129*, 8236–8246. (b) Spruell, J. M.; Paxton, W. F.; Olsen, J. C.; Benítez, D.; Tkatchouk, E.; Stern, C. L.; Trabolsi, A.; Friedman, D. C.; Goddard, W. A.; Stoddart, J. F. *J. Am. Chem. Soc.* **2009**, *131*, 11571–11580.

(19) In order to lend further support to our proposed multistep switching mechanism, we have carried out spectroelectrochemistry (see the Supporting Information, Figure S2) on the [3]catenane $\mathbf{1}^{4+}$. On applying a potential of +500 mV, formation of a characteristically broad NIR absorption band at 2000 nm, indicating the formation of the mixed-valence dimer, was observed. When the applied potential was increased to +800 mV, the formation of the radical-cation dimer, with its characteristic absorption band at 800 nm, was observed. Finally, increasing the applied potential to +1.2 V led to the formation of a broad absorption band at 600 nm as a result of charge transfer between $BIPY^{2+}$ units of the MS^{4+} cyclophane and the DNP units located within its cavity, in keeping with circumrotations on the part of both ring

components. It is important to note that the results of the chemical oxidations are completely in line with these observations made on the basis of spectroelectrochemistry.

(20) We can rule out the possibility of there being DNP···$TTF^{+\bullet}$ interactions inside the cavity of $\mathbf{MS}^{4+}$. In previous work (Ashton, P. R.; Balzani, V.; Becher, J.; Credi, A.; Fyfe, M. C. T.; Mattersteig, G.; Menzer, S.; Nielsen, M. B.; Raymo, F. M.; Stoddart, J. F.; Venturi, M.; Williams, D. J. *J. Am. Chem. Soc.* **1999**, *121*, 3951–3957), we have shown that mixing BDNP38C10 with the $TTF^{+\bullet}$ radical-cation does not result in any change in UV/Vis spectrum as a consequence of the absence of association. This observation was also verified by electrochemical experiments, indicating that the DNP···$TTF^{+\bullet}$ interaction is not a stabilizing one. Therefore, once one of the $TTF^{+\bullet}$ radical-cations leaves the cavity of the $\mathbf{MS}^{4+}$ ring, the other one is obliged to leave as well, resulting in two DNP units occupying the cavity of the $\mathbf{MS}^{4+}$ ring and becoming stabilized by CT interactions with the two $BIPY^{2+}$ units in the tetracationic cyclophane.

(21) Assuming that all of the species in the solution existed as $\mathbf{1}_{out}{}^{6+}$, the corresponding signal intensity would be doubled with respect to that of $\mathbf{1}^{5+}$ as a result of the 2-fold increase in the $TTF^{+\bullet}$ radical-cation concentration. Thus, the ratio of actual intensity to that of the hypothetical existence 100% of $\mathbf{1}_{out}{}^{6+}$ allows us to calculate the percentage populations of the state under equilibrium conditions.

(22) This proposed mechanism is also supported by the UV/vis/NIR experiments where the addition of 3.0 equiv of an oxidant resulted in a decrease in the absorption of the radical-dimer peak at 800 nm rather than disappearance of the radical-cation dimer peak. This result is an indication of disproportionation of $\mathbf{2}^{7+}$ to form $\mathbf{2}^{6+}$ and $\mathbf{2}^{8+}$.

(23) Attempts to crystallize the radical-cation dimer state, $\mathbf{1}^{6+}$, were hindered, we believe, by the equilibrium which exists in solution between $\mathbf{1}^{6+}{}_{in}$ and $\mathbf{1}^{6+}{}_{out}$. All attempts at crystallization of $\mathbf{1}^{6+}$ resulted in the isolation of tiny purple needles, a color reminiscent of the species $\mathbf{1}^{8+}$ wherein two DNP units are located inside the $\mathbf{MS}^{4+}$ ring so that there are no 'alongside' interactions with respect to the tetracationic cyclophane (See also Forgan, R. S.; Spruell, J. M.; Olsen, J.-C.; Stern, C. L.; Stoddart, J. F. *J. Mex. Chem. Soc.* **2009**, *53*, 134–138). These crystals did not diffract X-rays and so the solid-state structure could not be determined.

(24) The distance between two TTF units in each case is calculated by measuring the plane-to-plane distance. The angle of offset is defined by the relative orientations of the C-C double bonds in the TTF units. When these bonds are eclipsed, the angle is 0°. The vertical offset is the measure of offset between the planes of the TTF units, when these TTF units are in register, the vertical offset value is 0 Å. The hydrogen atoms and counterions have been omitted for clarity.

(25) Johnson, C. K.; Watson, C. R. *J. Chem. Phys.* **1976**, *64*, 2271–2286.

(26) This distortion has a significant effect on the central C═C bond length. In many cases in the literature, the length of this bond has been used as a diagnostic tool to determine the oxidation state of TTF units, but the unique environment provided by the mechanically interlocked molecule precludes the use of this measurement, on account of the effect of noncovalent bonding interactions on the TTF moieties in the two [3]catenanes.

(27) Wang, F. F.; Wang, Y.; Wang, B. Q.; Wang, Y. F.; Ma, F.; Li, Z. R. *Sci. China Ser., B: Chem.* **2009**, *52*, 1980–1986.

(28) Benítez, D.; Tkatchouk, E.; Yoon, I. I.; Stoddart, J. F.; Goddard, W. A. *J. Am. Chem. Soc.* **2008**, *130*, 14928–14929.

(29) (a) Zhao, Y.; Truhlar, D. G. *Theor. Chem. Acc.* **2008**, *120*, 215–241. (b) Zhao, Y.; Truhlar, D. G. *Acc. Chem. Res.* **2008**, *41*, 157–167.

(30) Zhang, Q.; Tu, Y. Q.; Tian, H.; Zhao, Y. L.; Stoddart, J. F.; Agren, H. *J. Phys. Chem. B* **2010**, *114*, 6561–6566.

(31) Spruell, J. M. *Pure Appl. Chem.* **2010**, *82*, 2281–2294.

(32) *Jaguar 7.6*; Schrodinger, LLC: New York: 2009.